Petrography and Physical Properties of Selected Rock Types Associated with the Hayward Fault, California

By Diane E. Moore[1] *and* David A. Ponce[1]

Open-File Report 01-263

2001

U.S. DEPARTMENT OF THE INTERIOR
U.S. GEOLOGICAL SURVEY

[1]Menlo Park, California

Contents

Introduction

This report provides brief petrographic descriptions of rock samples collected from the vicinity of the Hayward Fault, Northern California (Figure 1). Two groups of rock samples are represented here: 1) A set of six samples (H101, H102, H103, H107, H111, and H114) that were used for laboratory measurements of P- and S-wave velocity (Stanchits and Lockner, unpublished data), strength, density and porosity (Morrow and Lockner, 2001). This group was examined using standard petrographic microscope, scanning electron microscope (SEM) and electron microprobe techniques on polished thin sections. Analytical procedures for the electron microprobe and SEM work are the same as those reported by Moore (1997). 2) A larger group of samples, most of them 1"-diameter cores, on which density and magnetic susceptibility measurements were made as part of gravity and magnetic surveys of the Hayward Fault (Ponce and others, 1998). Because this second group of samples received less extensive laboratory study, examination of them was limited to standard petrographic microscope examination of covered thin sections. The density and susceptibility measurements of this second group of samples are included in this report. All sample locations are shown in Figure 2 and reported in the Appendix.

The petrographic descriptions are provided to help interpret the various physical measurements that have been made on the samples. The descriptions, therefore, generally include mention of any fabric elements present that may lead to anisotropy of some of the physical properties; these include compositional layering in gabbro, bedding planes in graywacke, and the density and orientation of fractures. The amounts of alteration and weathering were estimated, to help determine the degree to which the measured properties are representative of the original rock type. For example, basalt sample H107 has been so extensively altered that it bears little relation to the original volcanic rock. However, the chlorite + calcite + albite replacement assemblage could represent greenschist-facies modifications and thus reflect the present mineral assemblage of this rock unit at depth. Mineral or clast proportions were obtained from point counts, using a 1 mm x 1 mm grid. The number of points counted varies from sample to sample, with a minimum of ≈450 counts for some of the 1"-diameter samples.

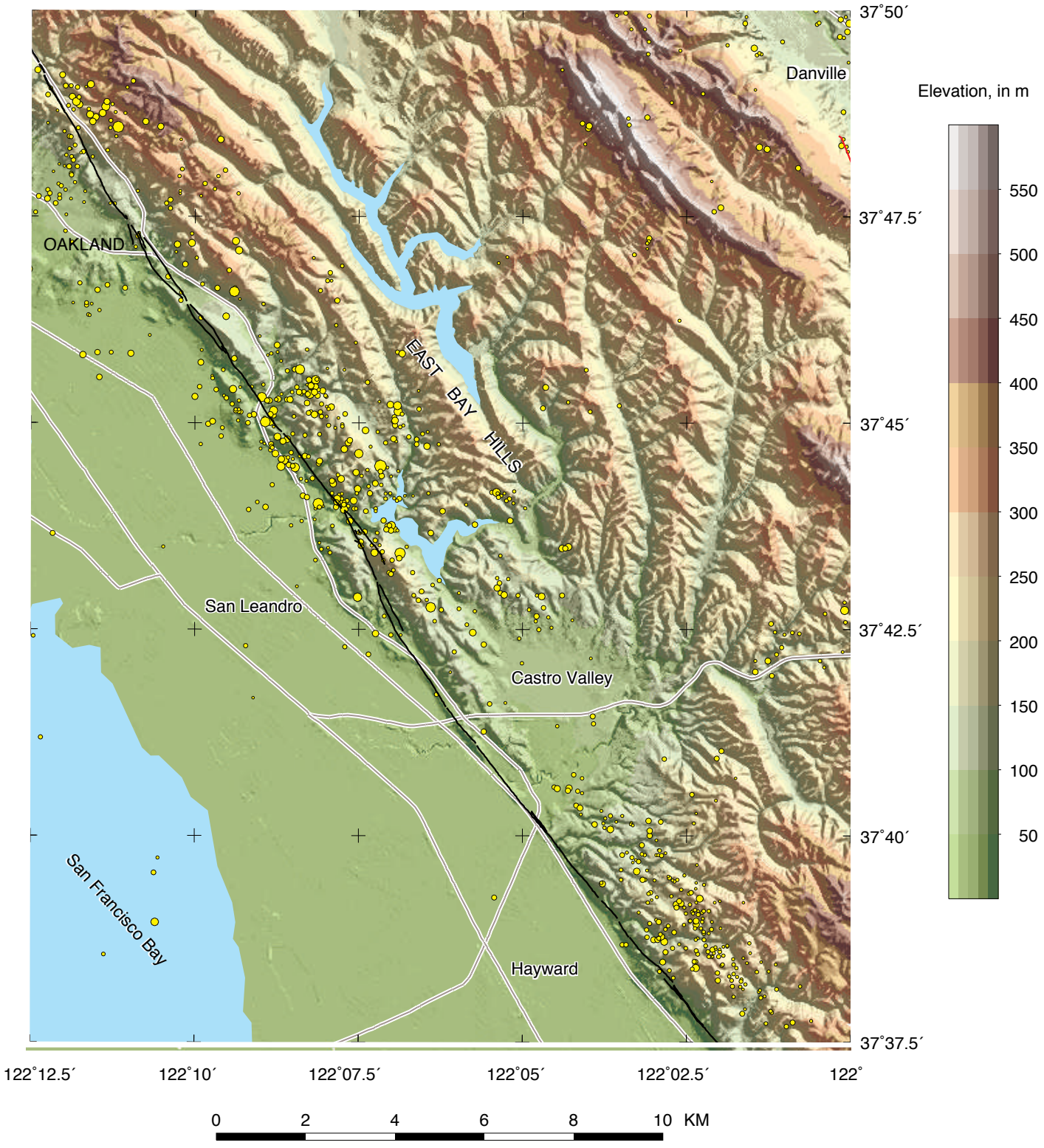

Figure 1. Shaded relief topographic map of the Hayward fault and vicinity showing seismicity (yellow circles). Seismicity data are from the U. S. Geological Survey's Northern California Seismic Net catalog from 1969 through September 23, 1999, M≥1.0. Black line, recent trace of Hayward fault from Lienkaemper and others (1991); gray lines, major highways and roads.

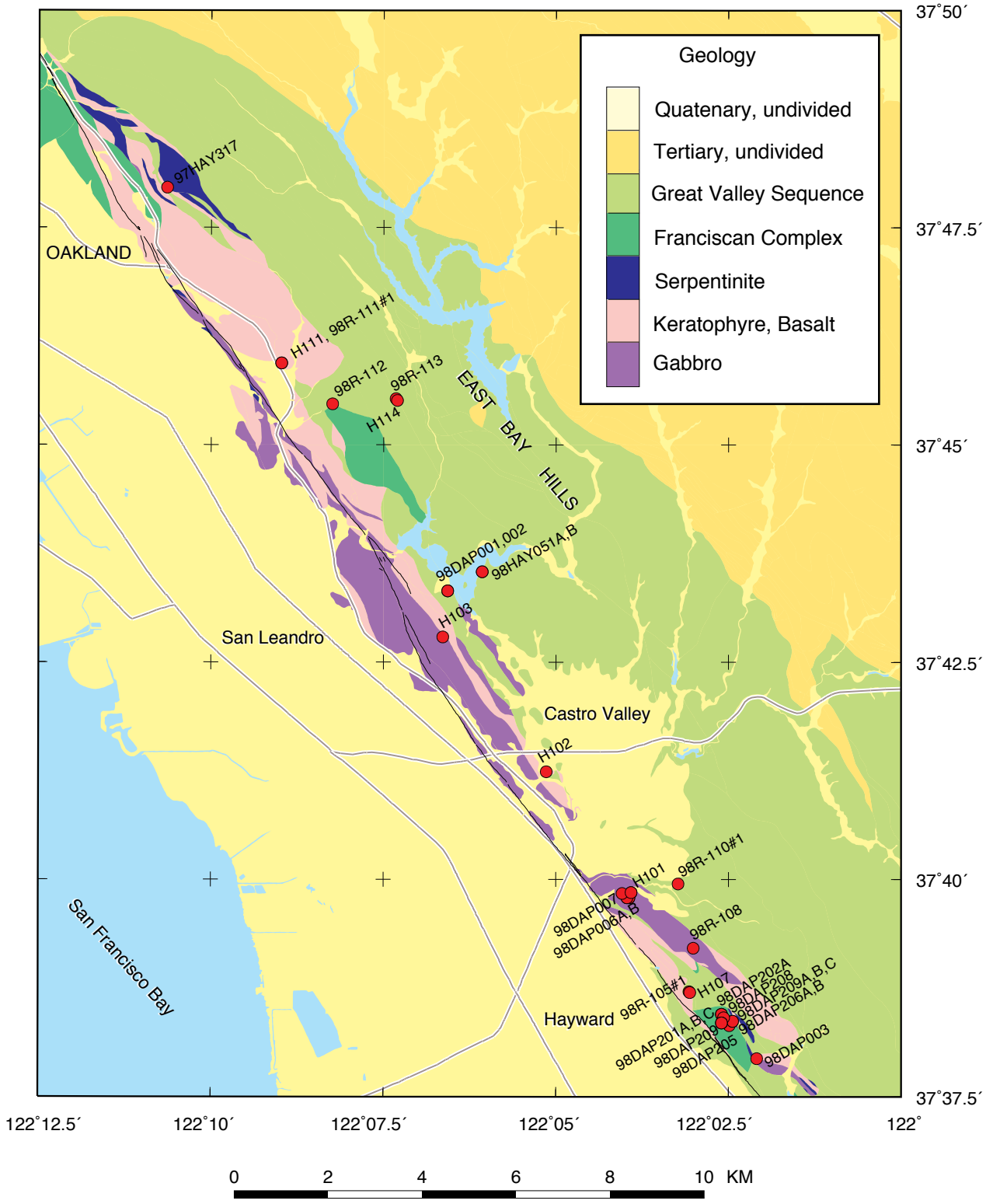

Figure 2. Rock sample locations. Geology modifed from Graymer (2000). Black line, recent trace of the Hayward fault from Lienkaemper and others (1991); gray lines, major highways and roads.

Igneous rocks are presented first, and they are grouped according to rock type. Sedimentary rock descriptions follow, and here the groupings are somewhat subjective. Three samples from the Cretaceous Joaquin Miller Formation are presented together, although one of the samples differ markedly from the other two. The remaining clastic sedimentary rocks are separated into groups of similar grain size and clast population.

Igneous Rocks

Gabbros

H101 Fine-Grained Gabbro

Table 1. H101–Mineral Proportions

Plagioclase	46.8
Amphibole	40.6
Magnetite*	8.2
Titanite	1.8
Clinopyroxene	0.9
Calcite	0.7
Chlorite	0.6
Zeolites	0.4
Total	100.0

* Includes some Ti-Fe oxides.

This gabbro (Table 1) is roughly equigranular, with grain sizes in the general range 0.50–0.85 mm diameter and reaching a maximum of 1.5 mm. The plagioclase, a bytownite averaging An_{85} in composition (Table 2), is very clean and has no traces of albitization. The principal mafic mineral in the gabbro probably was an augitic clinopyroxene (Table 2) that now occurs only as scattered, pale green relics. The pyroxene was subjected to extensive uralitic alteration, which involves replacement by aggregates of Ca-amphibole and which characteristically is a late magmatic process. Some of the amphibole aggregates are zoned, with darker blue-green crystals along the rims and paler green, more tremolitic amphiboles in the cores. The rim amphiboles also tend to be coarser-grained than those in the core, often forming a crystallographically continuous band around the crystal boundary. The cores contain aggregates of narrow, bladed amphiboles commonly arranged such that they preserve the twinning and/or cleavage patterns of the original pyroxene.

Table 2. H101 — Mineral Compositions

	Plagioclase			Clino-pyroxene	Amphibole		Chlorite			Titanite
	main	Na-rich cores	Ca-rich rims		paler green	darker green	main	lowest Fe	highest Fe	
SiO_2	47.07	47.64	45.71	51.55	53.49	50.13	24.92	27.03	24.40	30.52
TiO_2	0.01	0.01	0.01	0.41	0.22	0.36	0.04	0.04	0.07	37.97
Al_2O_3	33.95	33.17	34.80	2.34	2.44	5.04	19.71	19.81	19.19	1.55
Fe_2O_3	0.49	0.47	0.28	1.25	2.91	3.50	--	--	--	--
FeO	--	--	--	8.20	7.76	13.35	37.11	24.76	40.55	0.99
MgO	0.02	0.02	0.03	13.86	16.91	11.92	6.92	15.90	4.69	--
MnO	0.01	0.01	0.02	0.34	0.24	0.31	0.27	0.20	0.29	0.01
CaO	17.16	15.81	18.27	21.69	12.50	11.97	0.11	0.13	0.09	28.39
Na_2O	1.73	2.24	0.97	0.21	0.13	0.27	0.02	--	--	0.02
K_2O	--	0.01	0.01	--	0.01	--	--	--	--	--
BaO	0.01	0.02	0.01	NA	NA	NA	NA	NA	NA	NA
Cr_2O_3	NA	NA	NA	0.03	--	0.01	--	--	--	--
Total	100.45	99.40	100.11	99.88	96.61	96.86	89.10	87.87	89.28	99.45
Si	2.15	2.20	2.10	1.93	7.68	7.39	5.51	5.66	5.51	1.00
AlIV	1.83	1.80	1.89	0.07	0.32	0.61	2.49	2.34	2.49	--
AlVI	--	--	--	0.03	0.09	0.26	2.66	2.54	2.61	0.06
Ti	--	--	--	0.01	0.02	0.04	0.01	0.01	0.01	0.94
Fe^{+3}	0.02	0.01	0.01	0.04	0.31	0.39	--	--	--	--
Fe^{+2}	--	--	--	0.25	0.93	1.65	6.88	4.33	7.65	0.03
Mg	--	--	--	0.77	3.62	2.62	2.28	4.95	1.58	--
Mn	--	--	--	0.01	0.03	0.04	0.05	0.03	0.06	--
Ca	0.85	0.78	0.90	0.87	1.92	1.90	0.03	0.03	0.02	1.00
Na	0.15	0.20	0.10	0.02	0.04	0.08	--	--	--	--
K	--	--	--	--	--	--	--	--	--	--
Ba	--	--	--	NA	NA	NA	NA	NA	NA	NA
Cr	NA	NA	NA	--	--	--	--	--	--	--
O	8	8	8	6	23	23	28	28	28	5

Patches of chlorite and calcite in the centers of some altered pyroxenes represent a later, lower-temperature reaction than the uralitization process.

Magnetite principally occurs as separate, primary crystals that fill the interstices between plagioclase and pyroxene, or as fine-grained exsolved material associated with the altered mafic minerals. Small, euhedral crystals of Ti-Fe oxide occur with the magnetite.

A small number of cracks filled with secondary minerals such as chlorite, titanite, and calcite occur in various orientations. Some of these cracks have refractured and they are marked by reddish Fe-staining. This suggestion of weathering is very minor, however.

H103 Coarse-Grained Gabbro

Table 3. H103–Mineral Proportions

Plagioclase	50.2
Clinopyroxene	12.1
Orthopyroxene	11.6
Zeolite	8.6
Amphibole	6.5
Phyllosilicates*	6.3
Prehnite	3.8
Calcite	0.5
Magnetite	0.4
Total	100.0

*About one-fourth of this is pure chlorite. The remainder is a mixture of chlorite and other phyllosilicates.

Both the plagioclase and the pyroxenes in this two-pyroxene gabbro (Table 3) average 2–3 mm in length, with a maximum of 5 mm. In contrast to H101, the plagioclase has a very grainy appearance, whereas the pyroxenes are well preserved. The plagioclase (An_{90}; Table 4) crystals are crossed by many narrow, filled intragranular cracks, and traces of albite were identified during SEM examination. The clinopyroxene — a diopsidic augite (Table 4) — is distinguishable by its pale green color, fine-scaled twinning, and relatively high birefringence, the orthopyroxene — a bronzite (Table 4) — by its pale pink-to-green pleochroism and low birefringence, and the dark-brown alteration that is concentrated along internal cracks. Both pyroxenes show only minor replacement by amphiboles at their rims. The amphibole replacing orthopyroxene has slightly lower Ca contents and a slightly higher Fe/Mg ratio than that replacing clinopyroxene (Table 4), which is consistent with the compositional differences between the two pyroxenes. The scarce opaque minerals (Table 3) occur as small, euhedral inclusions in pyroxene and, to a lesser extent, in plagioclase. Veinlets of secondary Fe-oxides are associated with chloritic alteration. Small, red-stained patches surrounding a few of the Fe-oxides are the only evidence of weathering in this gabbro.

Table 4. H103 — Mineral Compositions

	Plagioclase	Clino-pyroxene	Ortho-pyroxene	Amphibole			Chlorite		Thom-sonite	Prehnite
				rims to cpx	with plag.	rims to opx	higher Mg	lower Mg		
SiO_2	45.86	53.01	53.83	49.75	51.94	51.68	27.73	27.02	40.96	43.33
TiO_2	0.01	0.15	0.16	0.97	0.48	0.13	0.01	0.01	0.01	0.01
Al_2O_3	34.48	1.25	1.30	6.49	4.51	4.30	20.12	20.35	30.18	24.33
Fe_2O_3	0.44	0.47	0.56	5.99	6.66	8.72	--	--	0.72	0.10
FeO	--	6.60	16.57	4.60	3.39	6.02	20.72	23.83	--	--
MgO	0.03	15.18	25.75	16.45	17.70	14.82	18.76	16.66	0.42	0.02
MnO	0.01	0.26	0.38	0.16	0.16	0.46	0.18	0.26	0.02	0.02
CaO	17.92	22.60	1.29	11.91	11.95	11.16	0.13	0.07	12.07	26.77
Na_2O	1.20	0.14	0.01	0.74	0.50	0.40	0.01	--	3.56	0.02
K_2O	0.03	--	--	0.06	0.04	0.03	--	--	--	--
BaO	0.02	NA	NA	NA	NA	NA	NA	NA	NA	0.01
Cr_2O_3	NA	0.09	0.04	0.12	0.08	0.05	--	0.01	0.01	NA
Total	100.00	99.75	99.89	97.24	97.41	97.77	87.66	88.21	87.88	94.60
Si	2.12	1.97	1.96	7.09	7.34	7.39	5.69	5.60	21.40	6.02
AlIV	1.87	0.03	0.04	0.91	0.66	0.61	2.31	2.40	--	1.98
AlVI	--	0.03	0.02	0.18	0.09	0.11	2.54	2.58	18.59	2.00
Ti	--	--	--	0.10	0.05	0.02	--	--	--	--
Fe^{+3}	0.02	0.01	0.02	0.64	0.71	0.93	--	--	0.28	0.01
Fe^{+2}	--	0.20	0.50	0.55	0.40	0.73	3.55	4.13	--	--
Mg	--	0.84	1.40	3.50	3.72	3.15	5.74	5.14	0.33	--
Mn	--	0.01	0.01	0.02	0.02	0.06	0.03	0.05	0.01	--
Ca	0.88	0.90	0.05	1.83	1.80	1.71	0.02	0.01	6.75	3.98
Na	0.10	0.01	--	0.21	0.14	0.11	--	--	3.61	--
K	--	--	--	0.01	0.01	--	--	--	--	--
Ba	--	NA	NA	NA	NA	NA	NA	NA	NA	--
Cr	NA	--	--	0.01	0.01	--	--	--	--	NA
O	8	6	6	6	23	23	28	28	80	22

This sample contains several sub-parallel, intergranular veins that are filled with prehnite and the zeolite mineral thomsonite (Table 4). The widest veins form a closely spaced set about 6–7 mm in width, and the gabbro adjoining this group of veins has been heavily altered. Much of the plagioclase in the band of altered gabbro has been replaced by thomsonite + prehnite, and the alteration along cleavages and cracks in the pyroxenes is more intense inside the band than outside.

Other Gabbros

(Samples: 98R-108; 98DAP-001; 98DAP-006A; 98DAP-006B; 98DAP-007; 98DAP-207.)

Table 5. Mineral Proportions and Physical Properties of Other Gabbro Samples

	98R-108	98DAP-001	98DAP-006A	98DAP-006B	98DAP-007	98DAP-207
Plagioclase	58.9	Tr	51.9	36.1	40.6	1.5
Fine-grained Alteration*	—	48.0	—	—	—	25.8
Clinopyroxene	15.2	35.0	3.4	1.3	14.4	28.2
Orthopyroxene	19.1	1.0	—	—	—	—
Amphibole	0.6	5.7	35.7	47.1	39.2	19.7
Opaques	4.5	0.7	2.0	2.3	0.8	1.9
Chlorite	0.8	6.3	6.8	7.1	2.3	20.2
Zeolites	0.6	—	0.2	3.8	0.2	—
Calcite	0.2	—	—	—	1.0	—
Prehnite	—	3.0	—	—	—	2.7
Titanite	—	0.3	—	1.5	1.5	—
White Mica	—	—	—	0.5	—	—
Epidote	—	—	—	0.3	—	—
Total	100.0	100.0	100.0	100.0	100.0	100.0
Grain Density (g/cm^3)	3.03	2.86	2.83	2.85	2.89	2.70
Sat. Bulk Dens. (g/cm^3)	3.02	2.86	2.79	2.82	2.86	2.68
Dry Bulk Dens. (g/cm^3)	3.02	2.81	2.77	2.80	2.85	2.67
Susceptibility (cgs x 0.001)	4.99	0.01	0.05	0.05	0.07	0.01

*Alteration of plagioclase to aggregates of chlorite + amphibole ± calcite ± sericite ± prehnite.

98R-108

This two-pyroxene gabbro (Table 5) has a layered texture consisting of coarse-grained plagioclase-rich zones that alternate with finer-grained, pyroxene-rich layers. Both the tabular plagioclase crystals and the accompanying pyroxenes in the plagioclase-rich zones reach 1.7 mm in length; pyroxenes in the pyroxene-rich bands average 0.4 mm diameter with a maximum of

0.95 mm. Some of the opaques appear to be primary igneous minerals, whereas other, probably secondary minerals are concentrated along the cleavages of partly altered pyroxenes. Two prominent sets of long, narrow, filled fractures are oriented at about 70–80° angles to each other, and the cracks typically occur in clusters of three to six. A third, subsidiary set of shorter cracks bisects the acute angle between the two main fracture sets, and this orientation is nearly perpendicular to the mineral layering. The rock looks unweathered.

This sample has the highest density of the 6 in Table 5, which is consistent with the good preservation of its three major igneous minerals: bytownite (density 2.70-2.75 g/cm^3), orthopyroxene (density 3.43 g/cm^3 for a mineral composition similar to that in Table 4), and clinopyroxene (density 3.37 g/cm^3 for a composition similar to those in Tables 2 and 4). Mineral densities are from Deer et al. (1962, v. 2 [pyroxenes] and v. 4 [plagioclase]). This sample also has by far the highest magnetic susceptibility of all those reported in this paper. This sample does have the highest opaque-mineral content of any of the gabbros in Table 5, and the lack of weathering features suggests that the igneous magnetite has not been oxidized.

98DAP-001

The clinopyroxene in this heavily altered gabbro is relatively well preserved except for networks of filled intragranular cracks, but the plagioclase has been almost completely replaced by a very fine-grained aggregate of minerals that include chlorite, sericite, calcite, and prehnite. Because it was almost impossible to identify the individual alteration minerals in the petrographic microscope, they are grouped together as "fine-grained alteration" in Table 5. That proportion approximates the original plagioclase content of the sample. The gabbro is not layered and the original grain sizes are relatively uniform, averaging ≈1.25 mm and reaching a maximum of 2 mm for plagioclase and clinopyroxene. Patches of pale-green, Mg-rich chlorite rimmed by amphiboles have replaced a mafic mineral, possibly either olivine or orthopyroxene. A few small, rounded, high-relief crystals, typically encased in plagioclase phenocrysts, may be relict orthopyroxenes. The rock contains numerous veins that may have formed at different times in its history. The older ones are as much as 0.5 mm wide and contain chlorite, amphiboles, and Fe-oxides. Several younger, prehnite-filled veins are also present. The sample is coming apart along some of these fractures, and weathering features are concentrated along them.

98DAP-006A

This rock resembles H101, the uralitized gabbro sample. The nearly equant plagioclase phenocrysts average 0.9 mm long but a few reach 2.25 mm. The plagioclase is well preserved, but it has a dusty, light-brown appearance in plane-polarized light, is extensively fractured, and appears to be partly albitized along the cracks. Individual pyroxene crystals were ≤1.7 mm long, but they commonly occurred in 6 mm-long clusters. Amphiboles replacing the larger pyroxene crystals form mats of interlocking, bladed crystals that vary in color from medium green to nearly colorless. The few opaque minerals present may all be secondary minerals associated with the amphibole-forming reactions. The sample is crossed by a throughgoing open fracture that contains small amounts of calcite and that is associated with incipient weathering features. Other cracks are filled with layers of brown Fe-rich material, chlorite, amphibole, and a possible zeolite.

98DAP-006B

This sample is very similar to 98DAP-006A with respect to grain size and alteration character. The largest plagioclase phenocrysts, at 1.7 mm long, are somewhat smaller than those in 98DAP-006A, but the average grain size is comparable, in the range 0.7–1 mm. These plagioclase phenocrysts also contain a dense network of intragranular cracks. Some wide (to 0.5 mm) prehnite-filled veins are cross-cut by narrow calcite-filled veins. The opaques (Fe ± Ti oxides) are very fine-grained and probably all secondary. Part of the edge of the cored cylindrical sample has broken off, and weathering features are concentrated along the break. Red stains surrounding some of the Fe-oxides in the rest of the sample are suggestive of incipient, pervasive weathering.

98DAP-007

This is a faintly layered, medium- to coarse-grained, partly uralitized gabbro. The long dimensions of tabular plagioclase crystals (to 3.0 x 0.9 mm in size) and elongate clinopyroxenes are aligned. The plagioclase has a dusty appearance caused by fine-grained inclusions, and the crystal boundaries are slightly recrystallized. Despite the abundance of secondary amphiboles, the clinopyroxenes are much better preserved than in 98DAP-006A and -006B. Two prominent sets of intergranular fractures filled with calcite + prehnite ± Fe-oxides are oriented subparallel and nearly perpendicular, respectively, to the layering. Some of these filled cracks have recently refractured, and weathered patches are distributed throughout the sample.

98DAP-207

This heavily altered gabbro is very similar to 98DAP-001. The clinopyroxenes are well preserved except for narrow fringes of bladed amphiboles along their rims, but nearly all the plagioclase has been thoroughly altered. In this case, many of the alteration products of the plagioclase are sufficiently coarse-grained to identify (Table 5). Much of the identifiable alteration is chlorite that has crystallized along the cleavage and twin planes of the plagioclase. Some of the plagioclase crystals were ≈4 mm long, and the clinopyroxene crystals are ≤2.75 mm long. The long dimensions of the largest crystals show a faint alignment. As with 98DAP-001, patches of pale green chlorite that are rimmed by amphiboles may have pseudomorphically replaced a mafic mineral other than clinopyroxene. Several filled, intergranular fractures cross the sample, and slivers of gabbro situated between closely spaced fractures are more heavily altered than the rest of the sample. One previously filled crack has refractured, and the rock adjacent to it is slightly weathered. This sample has the lowest density of the 6 gabbros in Table 5, which may be a function of its high chlorite content. Approximately two-thirds of this sample is secondary minerals.

Basalt

(Sample: H107).

Table 6. H107–Mineral Proportions

Plagioclase	28.4
Quartz	1.6
Chlorite	18.1
Calcite	40.9
Opaques	5.8
Titanite/Leucoxene	5.2
Total	100.0

H107

This relatively coarse-grained, vesicular basalt originally consisted of tabular plagioclase phenocrysts, 0.2–0.75 mm in length, set in a matrix rich in mafic minerals. However, the rock has been very heavily altered to a calcite + chlorite + albite assemblage (Table 6). The most calcic plagioclase relic is a labradorite (Table 7) of composition An_{58}. The rims of numerous plagioclase crystals have been albitized and the cores replaced by chlorite. Many other plagioclase phenocrysts have been replaced by clean, medium-grained calcite. The groundmass contains some 6-sided crystal outlines, about 20-30 μm in length, that probably were clinopyroxenes originally. A few <20 μm-wide pore spaces in the groundmass are partly filled with tiny, euhedral crystals whose crystal outlines and composition (Mg-Ca-Fe-Al silicate; this is a qualitative composition obtained during SEM analysis— see Moore, 1997) suggest that they may be amphiboles.

The walls of the vesicles in the basalt are lined with quartz crystals with euhedral terminations, and the centers of the vesicles are filled with clean calcite. A few randomly oriented, calcite-filled veins cut the basalt. One recently refractured vein is surrounded by a red-stained zone of weathered basalt that ranges from 1.5 to 5 mm in width.

Table 7. H107 — Mineral Compositions

	Plagioclase				Chlorite		
	highest Ca	partly altered	partly altered	albite	ground-mass	with plagioclase	reddish crystals
SiO_2	53.55	56.26	58.15	67.56	32.09	32.70	30.07
TiO_2	0.04	0.07	0.03	0.02	0.09	0.06	0.11
Al_2O_3	28.15	26.71	25.89	20.35	14.70	14.20	13.18
Fe_2O_3	0.93	0.82	0.79	0.28	--	--	--
FeO	--	--	--	--	23.93	24.75	28.40
MgO	0.11	0.07	0.05	0.04	15.39	14.56	12.93
MnO	0.04	0.02	0.01	0.01	0.34	0.30	0.26
CaO	11.81	9.65	8.28	0.39	0.95	0.75	0.73
Na_2O	4.43	5.61	6.28	11.08	0.05	0.10	0.19
K_2O	0.18	0.24	0.34	0.25	--	--	0.01
BaO	0.03	0.01	0.04	0.03	NA	NA	NA
Cr_2O_3	NA	NA	NA	NA	0.01	0.03	0.02
Total	99.27	99.46	99.86	100.01	87.55	87.45	85.90
Si	2.45	2.54	2.61	2.95	6.68	6.83	6.59
AlIV	1.51	1.43	1.37	1.05	1.32	1.17	1.41
AlVI	--	--	--	--	2.27	2.32	1.99
Ti	--	--	--	--	0.02	0.01	0.02
Fe^{+3}	0.03	0.03	0.03	0.01	--	--	--
Fe^{+2}	--	--	--	--	4.16	4.32	5.20
Mg	0.01	--	--	--	4.77	4.53	4.22
Mn	--	--	--	--	0.06	0.05	0.05
Ca	0.58	0.47	0.40	0.03	0.21	0.17	0.17
Na	0.31	0.50	0.54	0.95	0.02	0.04	0.08
K	0.01	0.02	0.02	0.01	--	--	--
Ba	--	--	--	--	NA	NA	NA
Cr	NA	NA	NA	NA	--	--	--
O	8	8	8	8	28	28	28

Tonalite and Tectonized Tonalite/Diorites

(Samples: tonalite, 98DAP-206A; possibly sheared and variably altered tonalite/diorite, 98DAP205 and 98DAP-206B.)

Table 8. Tonalite/Diorite Mineral Proportions and Physical Properties

	98DAP-206A	98DAP-205	98DAP-206B
Plagioclase	50.1	48.3	47.2
Quartz	22.1	16.1	8.6
Amphibole	4.4	—	4.9
Biotite	1.5	—	0.4
Opaques	0.4	4.2	4.7
Calcite	—	7.6	9.7
Chlorite	13.4	18.0	16.3
Titanite/Leucoxene	7.5	5.8	8.2
Apatite	0.6	—	—
Total	100.0	100.0	100.0
Grain Density*	2.70	2.65	2.60
Sat. Bulk Density	2.69	2.63	2.59
Dry Bulk Density	2.68	2.62	2.58
Susceptibility	0.03	0.20	0.02

*See Table 5 for units of the four physical properties.

These three samples illustrate different degrees of deformation and alteration of a compositionally variable tonalite/diorite plutonic body that perhaps was caught up in a shear or fault zone. Many of the deformation textures in these samples are similar to ones developed in granodiorite in the damage zone and gouge core of the active Nojima fault on Awaji Island, Japan (Moore and others, 2000).

98DAP-206A

In this hornblende-biotite tonalite (a tonalite is a quartz diorite in which the quartz content exceeds 10%; see Table 8), the largest plagioclase crystals are 2.25 mm long and patches of quartz reach 2 mm diameter. No traces of K-feldspar were found. The hornblende is anhedral and only slightly chloritized, whereas nearly all the biotite has been replaced by chlorite + titanite. The plagioclase has a grainy look that may represent sericitic alteration, although the coarsest-grained alteration patches in the plagioclase are all chloritic. This sample has been slightly deformed; in particular, the quartz is heavily fractured and partly polygonized. One possible shear of variable width (0.03 to 1.7 mm) crosses the sample; quartz and plagioclase that were ground up in this shear have partly recrystallized. For the most part, the shear follows crystal boundaries, but a narrow subsidiary strand cuts through and offsets a pair of twinned plagioclase crystals. A number of narrow, chlorite-filled fractures may also be shears or sheared veins, because the chlorite is oriented sub-parallel to the fracture walls in the manner of slip

fibers. The tonalite contains a few fresh-looking open cracks, but there is little evidence of weathering.

98DAP-205

On first viewing, this rock looked to be a very poorly sorted clastic rock (ranging from a clayey matrix to pebbles >20 mm long) whose detritus was derived largely from two plutonic bodies. However, closer examination reveals that it is, in fact, a heavily deformed plutonic body of variable composition. The principal textural/compositional facies is a biotite-hornblende tonalite similar to 98DAP-206A. This tonalite is somewhat finer-grained than the other sample; the largest quartz crystals are 1.5 mm in diameter, and the largest plagioclase crystals are 1.8 mm long. All the hornblende has been pseudomorphically replaced by chlorite + calcite and the biotite by chlorite + titanite/leucoxene. The second, less abundant facies is a diorite that consists largely of tabular plagioclase crystals ≤0.15 x 0.85 mm in size and hornblende that has been completely altered to calcite + chlorite. The diorite facies also contains some interstitial quartz crystals <0.25 mm long and a few chloritized biotites, making its composition not much different from that of the tonalite. The mineral proportions reported for this sample in Table 8 are for the entire thin section and correspondingly represent a mix of the two facies.

For the most part, these two rock types occur in different fragments separated by shears, but one 1–2 mm wide transition zone between the two facies was found in one fragment. Moving from the tonalite to the diorite, the quartz content decreases relatively abruptly with accompanying changes in the plagioclase textures and sizes, whereas the biotite begins to decrease about 1 mm closer to the diorite side.

An approximately 8 mm-wide shear at one end of the thin section contains lozenge-shaped pieces of the diorite in a finely ground matrix. This shear is cross-cut by a 0.03 mm-wide vein filled with calcite and either a fine-grained zeolite or albite. This sample contains no open fractures and no obvious signs of weathering.

98DAP-206B

At first glance, this sample has an even more pronounced detrital appearance than 98DAP-205, but this is owing to the ≈10 mm-wide band of coarse-grained "gouge" in the middle of the thin section. To one side of this gouge zone are large pieces (to ≈15 mm long) of the diorite, in which the plagioclase crystals are somewhat smaller and the amphiboles more abundant than in the diorite facies of 98DAP-205. On the other side of the gouge zone are fragments of tonalite that are nearly identical to that in 98DAP-205, but in addition there is one large (•20 mm long) piece of heavily altered and somewhat deformed tonalite. The alteration consists largely of the partial breakdown of the quartz to fine-grained aggregates, and the replacement of the plagioclase by interlocking aggregates of clean, bladed (albitic?) plagioclase.

Nearly all the fragments within the gouge layer are <2 mm diameter; one or two larger pieces have partly broken down along numerous fractures. The rock types identified among the gouge materials all correspond to the diorite, tonalite, and altered tonalite that are present on either side of the gouge layer. The deformation features are overprinted by an episode of calcite crystallization. Some of the calcite is associated with a greenish-brown sheet silicate that may be a silica-rich chlorite. Small veins filled with brownish chlorite ± calcite cut across the gouge.

A few small patches of crystals in the calcite may be a zeolite mineral, and euhedral Fe-oxides are associated with the brownish chlorite. New fractures have formed along some of the shears and veins.

Densities of the three tonalite/diorite samples (Table 8) decrease with increasing degrees of deformation and alteration. The very different magnetic susceptibilities of 98DAP-205 and 98DAP-206B suggests that their opaque-mineral contents are different, the higher susceptibility being correlated with higher magnetite content, and the lower value with a predominance of hematite and/or Fe-Ti oxides.

Keratophyre

(Samples: keratophyre, H111; altered keratophyre, H102.)

H111

The keratophyre consists of irregularly shaped quartz and feldspar phenocrysts, mostly 0.1–0.6 mm long, along with a number of lithic fragments that can reach several mm in length, which are all set in a fine-grained, partly recrystallized, quartzofeldspathic groundmass. The crystals and lithic fragments are packed closely together, and recrystallization processes have corroded some of their edges and generated overgrowths on others. No attempt was made to determine mineral abundances in this sample, because of the difficulty in distinguishing quartz from feldspar in the groundmass.

The keratophyre contains only a small percentage of other minerals, including chlorite and a K-bearing phyllosilicate whose composition (Table 9) is comparable to hydromuscovite analyses reported by Deer et al. (1962, vol. 3). The chlorite forms aggregates of 25-μm long platelets, and the K-phyllosilicate is associated with a TiO_2 mineral. Small crystals of iron-rich epidote (Table 9) are scattered throughout the rock, and trace minerals include pyrite, Ti-Fe oxides, Cu-S- and Cu-Fe-S-bearing phases, titanite, barite, and a Fe-O-bearing mineral. The latter mineral is concentrated along narrow cracks that have no preferred orientation.

A weathered zone covering about one-fourth of the thin section is characterized by red-stained chlorite and other mafic minerals and the presence of bright red and bright yellow grains that probably are hydrated Fe-oxides. Mafic minerals in the remaining three-fourths of the thin section are also faintly discolored.

Physical-property measurements were made on another sample of this keratophyre (98R-111). Density measurements (in g/cm^3) are 2.60 for grain density, 2.60 for saturated bulk density, and 2.59 for dry bulk density. The density measurements are consistent with the predominance of quartz (2.65 g/cm^3), K-feldspar (2.55–2.62 g/cm^3), and oligoclase (2.63–2.66 g/cm^3; these mineral densities are from Deer et al., 1962, v. 4). The sample had zero magnetic susceptibility, which is consistent with the scarcity of Fe-O-bearing minerals in the rock and the probability those present are all hydrated phases.

Table 9. H111 — Mineral Compositions

	K-feldspar	Oligoclase		Albite		Chlorite	K-bearing	Epidote
		most Ca-rich	main	main	most Na-rich	in altered plagioclase	Phyll.*	tiny pieces
SiO_2	64.50	3.05	64.85	66.79	67.95	34.48	49.97	37.49
TiO_2	--	--	--	0.01	0.01	0.03	0.03	0.24
Al_2O_3	18.48	23.29	21.84	20.87	20.03	21.31	34.74	25.10
Fe_2O_3	0.04	0.23	0.23	0.12	0.04	--	--	11.01
FeO	--	--	--	--	--	14.08	1.48	--
MgO	--	--	--	--	--	15.55	0.74	0.03
MnO	--	0.01	0.01	--	--	0.22	0.02	0.86
CaO	0.02	4.28	2.68	1.24	0.46	0.03	0.13	21.75
Na_2O	1.96	8.80	9.46	10.58	11.30	0.09	0.75	0.02
K_2O	13.45	0.47	0.69	0.54	0.35	0.02	4.22	--
BaO	0.24	0.04	0.06	0.05	0.03	NA	NA	0.02
Cr_2O_3	NA	NA	NA	NA	NA	0.03	--	NA
Total	98.69	100.17	99.82	100.20	100.17	85.84	92.08	96.52
Si	2.99	2.71	2.86	2.92	2.97	6.80		2.97
AlIV	1.01	1.21	1.14	1.08	1.03	1.20		0.03
AlVI	--	--	--	--	--	3.76		2.36
Ti	--	--	--	--	--	--		0.01
Fe^{+3}	--	0.01	0.01	0.01	--	--		0.67
Fe^{+2}	--	--	--	--	--	2.32		--
Mg	--	--	--	--	--	4.57		--
Mn	--	--	--	--	--	0.04		0.06
Ca	--	0.20	0.13	0.06	0.03	0.01		1.89
Na	0.18	0.75	0.81	0.90	0.96	0.04		--
K	0.80	0.03	0.04	0.03	0.01	--		--
Ba	0.01	--	--	--	--	NA		--
Cr	NA	NA	NA	NA	NA	--		NA
O	8	8	8	8	8	28		12.5

*No structural formula calculation was attempted, because of the variability of the hydromuscovite chemical formula (Deer et al., 1962), particularly with respect to H_2O-content.

H102

Whereas phenocrysts and lithic fragments are well preserved in H111, in this sample heavy alteration has almost completely obliterated the original granular texture. No feldspar phenocrysts remain, and only one or two small quartz crystals may be original. Only faint traces of the former crystal and lithic-fragment outlines can be seen; these tend to be marked by a faint dusting of Fe- and/or Ti-oxides at the rims. Overall, this is a fine-grained, quartz-rich rock; any plagioclase that may have been present has been removed but some possible K-feldspar was identified during SEM examination. Numerous veinlets of quartz cross-cut the rock in all directions. The coarsest-grained quartz — at 0.15 mm diameter —occurs in these veins and in a few patches in the groundmass. Some pore spaces were identified in the groundmass during SEM examination, but these may represent isolated rather than connected porosity. Quartz crystals lining the walls of the pores have euhedral outlines.

Fe- and Ti-oxides are scattered throughout the groundmass. In addition, bands of Fe- or Ti-oxides with dendritic shapes are bordered by a vermicular, Si-Al-bearing mineral that is probably kaolinite. The only other minerals identified were traces of apatite associated with the kaolinite and one crystal of pyrite. Because of the fine-grained character and heavy silicification of the rock, neither a point count nor microprobe analysis of the sample was attempted.

Partly Serpentinized Ultramafic Rocks

(Samples: 98DAP-002 and 97HAY317.)

Table 10. Ultramafic Rock Mineral Proportions and Physical Properties

	98DAP-002	97HAY317
Serpentine	38.2	17.9
Opaque Minerals	10.0	3.9
Clinopyroxene	46.5	71.3
Olivine	0.3	—
“Alteration”	5.0	6.9
Total	100.0	100.0
Grain Density*	2.88	3.06
Sat. Bulk Density	2.85	3.03
Dry Bulk Density	2.83	3.01
Susceptibility	0.30	0.00

*See Table 5 for units.

98DAP-002

This coarse-grained ultramafic rock probably was a peridotite. Although nearly all the olivine has been replaced by serpentine, much of the clinopyroxene is preserved. The olivines formed

clumps of crystals that together exceeded 7 mm in length. Individual clinopyroxene crystals are ≈3 mm long, and their long dimensions are modestly aligned. Approximately three-fourths of the serpentine in this sample (Table 10) replaces olivine; this serpentine is a greenish color and may be lizardite (see, for example, chapter 2 of O'Hanley, 1996). The serpentine filling veins is nearly colorless, commonly with a fibrous character, and may be chrysotile. The most prominent serpentine-filled fractures are sub-parallel, and they have numerous, nearly perpendicular offshoots. The clinopyroxenes contain many randomly oriented intragranular cracks. Scattered euhedral magnetite crystals may be primary minerals, but most of the Fe-oxides are by-products of the serpentinization of the olivine. Some very fine-grained alteration minerals could not be identified in thin section and they are listed in Table 11 as "alteration". This alteration is concentrated in narrow, irregular bands around the edges of clinopyroxene crystals, and it may represent the pseudomorphic replacement of a specific, interstitial mineral. Some patches of serpentine with deep blue-black interference colors have similar outlines to these bands, and the grainy alteration material may therefore be extremely fine-grained serpentine.

97HAY317

This clinopyroxenite is also a coarse-grained rock, with equant clinopyroxenes as large as 5 mm diameter. Nearly half the serpentine in the sample appears to replace olivine (8.7% out of the 17.7% listed in Table 10); the remainder fills veins and occurs in bands in the pyroxene. As with 98DAP-002, the greenish serpentine replacing olivine may be lizardite, and the colorless serpentine with a fibrous habit filling veins may be chrysotile. The olivine crystals averaged 0.5–0.6 mm diameter and reached a maximum of 1.2 mm in length. Most of the olivine occurred as single crystals interstitial to the clinopyroxenes, but a few small clusters of olivine crystals were also present. The opaque mineral content is less than half that of 98DAP-002, because of the smaller original olivine content. This sample also contains some very fine-grained, unidentifiable alteration minerals. The sample is coming apart along fractures with associated weathering features.

The higher density of 97HAY317 compared to 98DAP-002 is a result of its lower serpentine-mineral content (density ≈2.5 g/cm^3, Deer et al., 1962, v. 3).

Sedimentary Rocks

Sandstones and Carbonate-Rich Rock, Joaquin Miller Formation

(Samples: H114; 98R-113; 98R-110.)

Samples 98R-110 and 98R-113 are described with H114 in this section, because they also come from the Cretaceous Joaquin Miller Formation of the Great Valley Sequence. 98R-113 and H114 are very similar in texture and clast composition, whereas 98R-110 differs significantly from the other two. A point count of 98R-110 was not made.

Table 11. Joaquin Miller Sandstone–Clast Content and Physical Properties

	H114	98R-113	98R-110
Lithic Fragments:			
Volcanic	15.6	10.1	Not
Plutonic	6.6	5.8	Made
Metasedimentary	8.4	8.8	
Sedimentary	1.7	3.7	
Calcite*	2.0	Tr	
Single-Crystal Clasts:			
Quartz	24.2	25.9	
Plagioclase	11.7	11.2	
K-feldspar	11.4	16.4	
Biotite	1.7	4.5	
Chlorite	1.3	0.4	
Muscovite	0.6	—	
Opaques/Heavy Minerals	0.7	—	
Matrix**	14.1	13.2	
Total	100.0	100.0	
Grain Density (g/cm^3)		2.53	2.68
Saturated Bulk Density (g/cm^3)	Not	2.42	2.67
Dry Bulk Density (g/cm^3)	Made	2.35	2.66
Susceptibility (cgs x 0.001)		0.01	0.02

*This calcite appears to be a secondary mineral, completely replacing the minerals in the original clasts. Tr = Trace amount. **Material counted as matrix in the sedimentary rock samples comprises all interstitial minerals, both detrital and secondary.

H114

The largest clasts in this rock are about 0.95 mm long; no alignment of grain shapes nor any other features suggestive of bedding were visible in the plane of the thin section. The rock is not very quartz-rich; rather, it contains many feldspar clasts (both plagioclase and K-feldspar) and a large lithic-fragment component consisting largely of volcanic and lesser plutonic igneous clasts and quartzose metasedimentary grains (Table 11). The matrix material includes calcite, narrow bands of Fe-oxides, chlorite, phengitic white mica (Table 12), possible kaolinite, and titanite and other Ti-bearing minerals such as leucoxene. Only small amounts of unfilled pore space remain. Of the mineral compositions reported in Table 12, the albite, the phengite, and all but one of the chlorite analyses represent secondary minerals whereas the others are for detrital minerals.

Fracturing is restricted to transgranular or intragranular cracks in single-crystal clasts, usually quartz. One of the transgranular cracks is filled with calcite, and a few contain tiny apatite crystals. The crack walls in several quartz grains have a spongy or etched appearance. The sample contains no obvious weathering features.

Table 12. H114 —Mineral Compositions

	Plagioclase			K-feldspar	Muscovite		Phengite
	clast	clast	secondary	clast	clast	clast	matrix
SiO_2	57.89	63.23	67.25	64.09	45.77	46.70	49.29
TiO_2	0.01	0.03	0.01	0.01	1.05	0.29	0.15
Al_2O_3	26.08	22.88	20.33	18.34	36.10	35.76	32.29
Fe_2O_3	0.15	0.24	0.04	0.10	1.34	0.48	2.22
FeO	--	--	--	--	--	--	--
MgO	--	--	--	--	0.59	1.07	1.61
MnO	0.01	--	0.01	0.01	0.02	0.01	0.01
CaO	8.00	3.97	0.70	0.02	0.01	0.03	0.06
Na_2O	6.91	9.13	11.00	0.46	1.15	0.45	0.15
K_2O	0.13	0.36	0.19	15.74	9.43	10.30	10.03
BaO	0.05	0.07	--	0.27	NA	NA	NA
Cr_2O_3	NA	NA	NA	NA	0.11	0.02	0.01
Total	99.23	99.91	99.53	99.04	95.57	95.11	95.82
Si	2.61	2.80	2.95	2.99	6.07	6.18	6.48
AlIV	1.39	1.19	1.05	1.01	1.93	1.82	1.52
AlVI	--	--	--	--	3.72	3.76	3.48
Ti	--	--	--	--	0.05	0.03	0.01
Fe^{+3}	--	0.01	--	--	0.13	0.05	0.22
Fe^{+2}	--	--	--	--	--	--	--
Mg	--	--	--	--	0.12	0.21	0.32
Mn	--	--	--	--	--	--	--
Ca	0.39	0.19	0.05	--	--	--	0.01
Na	0.60	0.79	0.94	0.05	0.30	0.11	0.04
K	0.01	0.02	0.01	0.94	1.60	1.74	1.68
Ba	--	--	--	0.01	NA	NA	NA
Cr	NA	NA	NA	NA	0.01	--	--
O	8	8	8	8	22	22	22

Table 12, continued.

	Chlorite					Biotite
	possibly detrital	replaces biotite	replaces biotite	replaces biotite	matrix	
SiO_2	25.86	26.23	29.34	31.27	31.52	33.58
TiO_2	0.07	0.28	0.12	0.07	0.01	2.45
Al_2O_3	21.96	21.48	23.14	21.42	19.57	20.28
Fe_2O_3	--	--	--	--	--	--
FeO	23.95	28.61	17.91	24.44	14.69	20.50
MgO	14.75	10.24	16.05	9.01	19.55	7.62
MnO	0.43	0.27	0.12	0.11	0.26	0.28
CaO	0.04	0.15	0.09	0.55	0.50	0.21
Na_2O	0.02	0.02	0.03	0.05	0.06	0.08
K_2O	--	0.30	0.05	0.19	0.14	7.53
BaO	NA	NA	NA	NA	NA	NA
Cr_2O_3	0.02	0.05	0.03	0.07	0.01	0.04
Total	87.10	87.63	86.88	87.18	86.31	92.57
Si	5.44	5.62	5.91	6.47	6.94	5.25
AlIV	2.56	2.38	2.09	1.53	1.06	2.75
AlVI	2.89	3.05	3.40	3.70	4.02	0.99
Ti	0.01	0.04	0.02	0.01	--	0.29
Fe^{+3}	--	--	--	--	--	--
Fe^{+2}	4.22	5.13	3.02	4.23	2.70	2.68
Mg	4.62	3.27	4.82	2.78	3.60	1.79
Mn	0.08	0.05	0.02	0.02	0.05	0.04
Ca	--	0.03	0.02	0.12	0.12	0.04
Na	--	--	0.01	0.02	0.02	0.02
K	--	0.08	0.01	0.04	0.04	1.50
Ba	NA	NA	NA	NA	NA	NA
Cr	--	0.01	0.01	0.01	--	--
O	28	28	28	28	28	22

98R-113

Compared to H114, this sample contains more clasts of K-feldspar and biotite, fewer volcanic lithic fragments, and almost no calcite (Table 11). Both the plagioclase and K-feldspar clasts are partly altered; in particular, some of the K-feldspar has been replaced by chessboard albite (Moore and Liou, 1979). The volcanic detritus includes a number of felsic to intermediate rock types. Quartz and feldspar grains are very angular; the largest such clasts are 0.75 mm long. The largest biotites and shaly fragments are 1.25 mm long and about one-fifth as wide as they are long, and a faint, possible bedding direction is defined by the preferred orientation of those clasts. The matrix consists largely of phyllosilicate minerals and grainy Fe-oxides, probably hematite.

One narrow, open crack crosses the sample, and a few short, open cracks are also present. These cracks tend to follow grain boundaries, except where they separate the cleavage planes of biotite. Except for the biotite, the clasts themselves are not significantly cracked: one fracture refracts through three adjoining grains, and a few intragranular and transgranular cracks have nucleated at high-stress points. These latter cracks are all filled with material injected from the matrix. Some of the Fe-oxides appear to be weathering.

98R-110

In contrast to the other two samples in this group, 98R-110 consists principally of fine-grained, grainy calcite that contains a scattering of small clasts (including Fe-oxides) and possible organic material. The sample may have been part of a concretion (R. Graymer, personal communication, 2001). The clasts are principally single-crystal quartz and feldspar grains and fine-grained metasedimentary rocks; they are generally 0.02–0.04 mm in diameter and the largest are only about 0.1 mm long. Veins of clean calcite cross the sample in two, nearly perpendicular directions, and both vein sets have a crack-seal character. The one set is ≈0.65 mm wide overall, and it contains 24 calcite bands. The other, perpendicular set of 37 bands is subdivided into smaller groups of bands that splay as they traverse the thin section. The individual crack-seal bands are all ≤0.03 mm wide. No open cracks were observed. A prominent zone of weathering on one side may be part of a weathering rind.

The somewhat higher density of this sample compared to 98R-113 (Table 11) is consistent with the higher density of the mineral calcite (2.72 g/cm^3; Deer et al., 1966) compared to the quartz and feldspars that make up more than one-half of the other sandstone sample.

Conglomeratic Clastic Rocks Rich in Igneous Detritus

(Samples: 98DAP-209A; 98DAP-209B; 98DAP-209C.)

This group of coarse-grained clastic sedimentary rocks is largely composed of mafic to intermediate igneous detritus. The mafic minerals have been heavily chloritized, and all the hand specimens have a greenish tinge. Because of the predominance of igneous detritus as well as the difficulty of distinguishing between grains and matrix in some places, the mineral content rather than the clast content of each sample was counted (Table 13).

Table 13. Mineral Proportions and Physical Properties of Volcanic-Rich Clastic Rocks

	98DAP-209A	98DAP-209B	98DAP-209C
Plagioclase	41.2	43.6	37.4
Quartz	0.7	2.5	0.8
Chlorite	23.1	25.1	19.6
Opaques	9.7	8.6	11.9
Calcite	17.1	13.0	24.3
Titanite/Leucoxene	7.8	7.0	5.8
Amphibole	0.2	0.2	—
Sericite	0.2	—	0.2
Biotite	—	—	—
Total	100.0	100.0	100.0
Grain Density*	2.62	2.60	2.64
Sat. Bulk Density	2.59	2.55	2.61
Dry Bulk Density	2.57	2.51	2.58
Susceptibility	0.26	0.17	0.20

*See Table 11 for units.

98DAP-209A

This is a coarse-grained (many clasts are 2–4 mm diameter) sandstone/conglomerate that consists largely of mafic to intermediate volcanic detritus of various types. These include many porphyritic volcanics (andesites and/or basalts) consisting of scattered plagioclase phenocrysts in a felted groundmass of tiny plagioclase blades and mafic minerals; aphanitic basalts/andesites; a few fine-grained dacitic volcanics; and vesicular basalts. Pieces of altered tonalite identical to that in 98DAP-206B are present, along with clasts of single-crystal plagioclase containing many chloritized inclusions. In addition, a small number of quartzite clasts (metasandstones) and a few fossil fragments were identified. The rock is very tightly packed and the interstices are filled with calcite, opaque minerals, and chlorite; chlorite crystallization tends to obscure the clast-matrix boundaries. Some interstitial patches of fine-grained quartz also appear to be secondary, pore-filling minerals. A considerable amount of chlorite and calcite also replace minerals in the clasts and fill fractures. A few open cracks may be recent features. Red staining indicative of incipient weathering is concentrated around some of the chlorite.

98DAP-209B

This sample is almost identical to 98DAP-209A, but it contains a few considerably larger (•12 mm diameter) pebbles and more than three times the amount of quartz as 98DAP-209A (Table 13). Most of the quartz is contained in the lithic fragments, but a few patches of medium- to fine-grained secondary quartz fill pore spaces, as was also observed in 98DAP-209A. The rock contains short, calcite-filled cracks and other, open cracks that may be of relatively recent origin.

Reddish and yellowish stains surrounding chlorite and Fe-oxides and associated with one of the larger open fractures are likely weathering features.

98DAP-209C

Of the three samples in this group, this one is the most heavily veined and it has the highest opaque-mineral content (Table 13). The largest veins reach 0.25 mm in width, and they are filled with clean calcite ± chlorite ± quartz (or albite), with the chlorite and quartz lining the vein walls and calcite in the centers. The rims of several of the volcanic-rock lithic fragments have recrystallized to fine-grained feldspar/quartz assemblages with a border of Fe-oxides. The largest clasts in this sample excees 8 mm in length; many of them are 2–3 mm in diameter. A few narrow, irregular, open cracks are present, but there are no obvious signs of weathering.

The three samples in this group have similar densities as well as similar, relatively high susceptibility values. The susceptibilities probably are associated with the presence of magnetite in the mafic volcanic detritus that predominates in all three.

Graywackes

(Samples: 98R-105; 98R-112; 98DAP-0030; 98DAP-201A; 98DAP-201B; 98DAP-201C; 98DAP-208.)

Table 14. Clast Contents and Physical Properties of Graywacke Samples

	98R-105	98R-112	98DAP-0030	98DAP-201A	98DAP-201B	98DAP-201C	98DAP-202A	98DAP-208
Lithic Fragments								
Volcanic	44.2	33.9	47.8	44.3	56.2	48.0	47.4	56.2
Plutonic	1.3	2.8	5.4	1.3	1.5	0.9	0.8	2.4
Metasedimentary	0.9	15.0	0.5	0.4	0.9	1.1	0.6	3.2
Sedimentary	—	3.0	1.0	2.2	1.1	—	0.4	4.1
Fossils (calcite)	2.4	Tr	Tr	5.2	3.7	4.5	—	1.5
Single-crystal Clasts								
Quartz	1.1	6.1	0.6	1.1	0.5	1.1	0.6	3.0
Plagioclase	24.2	10.8	19.0	18.5	12.8	18.5	23.0	9.6
Chloritized mafics*	10.2	10.2	7.0	12.4	12.1	11.1	4.8	2.1
Opaques	—	0.6	1.9	0.7	—	2.4	5.0	2.1
Pyroxene	—	—	—	0.2	—	0.2	—	—
K-feldspar	—	1.7	—	—	—	—	—	0.2
White Mica	—	—	—	—	—	—	—	0.2
Matrix	15.4	15.9	11.6	13.7	11.2	12.2	17.4°	15.4
Total	100.0	100.0	100.0	100.0	100.0	100.0	100.0	100.0
Grain Density**	2.48	2.56	2.67	2.61	2.59	2.63	2.64	2.61
Sat. Bulk Density	2.43	2.54	2.64	2.57	2.54	2.62	2.58	2.53
Dry Bulk Density	2.40	2.52	2.62	2.55	2.51	2.62	2.55	2.49
Susceptibility	0.03	0.02	0.90	0.04	0.03	0.04	0.06	0.04

*The grains probably were pyroxene and olivine originally. **See Table 11 for units. °Includes 0.8% of vein calcite.

98R-105

This sample comes from the volcanic breccia member of the Knoxville Formation (Kjkv of Graymer, 2000), which is locally the basal unit of the Great Valley Sequence. It is a dense, red-stained, poorly sorted graywacke, whose clasts are moderately well rounded but have low sphericity. Maximum grain size is ≈1.5 mm, and a faint bedding is defined by the aligned long dimensions of the clasts and fossil shell fragments. The detritus is largely derived from mafic igneous sources and consists principally of aphanitic volcanic lithic fragments, plagioclase crystals, and chloritized mafic grains. Some of the mafic grains contain relics of clinopyroxene; others may have been olivine originally (or serpentinized olivine) based on the textures of the chlorite; and a few probably were magnetite. Some of the pyroxenes are partly replaced by calcite rather than chlorite. Quartz is scarce, either as separate crystals or in lithic fragments (Table 14). The matrix is rich in chlorite + calcite + Fe-oxides (probably hematite, because of the moderately low susceptibility value), along with a few possible zeolites that form sprays of crystals filling pore spaces. The sample is crossed by a number of short, narrow calcite-filled cracks and one nearly 1.2 mm-wide calcite vein. A few jagged, open cracks are also present.

The density of this sample is the lowest of those in Table 14, but all eight sets of values are relatively close to each other and comparable to the densities of the other sandstone/graywacke samples (for example, Table 11 and Table 15).

98R-112

This graywacke sample comes from the conglomerate member of the Knoxville sandstone (Kjkc of Graymer, 2000). The presence of some single-crystal quartz clasts and quartzose metasandstone clasts help make this the most quartz-rich rock of the eight in Table 14. Although the volcanic lithic fragments are largely mafic, several fine-grained dacitic clasts are also present. A few extremely fine-grained lithic fragments may possibly be cherts rather than volcanic rocks. Grain size varies across the sample; an 8-mm wide layer on one side is relatively fine-grained, with a maximum clast length of ≈0.9 mm and with about three-fourths of the clasts being <0.4 mm in diameter. The maximum grain size in the rest of the sample is ≈1.25 mm, and about 30–40% are roughly 0.6 mm in diameter. The matrix differs from that of 98R-105 in that calcite is nearly absent (Table 14). Some of the chlorite in the matrix has grown into the pore spaces from grain walls. A few narrow (0.015 mm wide) dilational fractures are filled with quartz. One open, red-stained fracture crosses the sample, and other weathered-looking patches are scattered throughout it.

98DAP-0030

This third Knoxville sample (KJkv) is a poorly sorted rock whose overall grain size is ≤0.5 mm in diameter, but which contains scattered pebbles to 7.5 mm in diameter. The largest pebble is a dacitic volcanic rock, and several other pebbles are tonalitic plutonic rocks containing plagioclase + quartz + chloritized biotite ± epidote. This sample has the highest plutonic-clast content of the eight in this group (Table 14), and it also contains a number of unaltered clinopyroxene clasts to 1.5 x 0.75 mm in size. The other lithic fragments are predominantly

felsic to intermediate volcanic rocks. Based on their textures, a few of the chloritized mafics may have been olivine originally. Most of the quartz in the sample is contained in the pebbles of tonalite and metasedimentary rock; very little quartz (0.6%; Table 14) occurs as single-crystal grains. The graywacke also contains fragments of calcareous fossil shells, and a faint bedding direction is defined by the alignment of elongate shell fragments, some of the large clinopyroxenes, and the more elongate pebbles. A number of fresh-looking, randomly oriented, open cracks cross the sample. The hand specimen is variably red stained, and the thin section shows a moderate degree of weathering, somewhat less than that observed in 98R-105.

The very high susceptibility value for this sample in comparison to the other seven in Table 14 is not obviously explained by its appearance under the petrographic microscope. Sample 98DAP-208, for example, contains at least as many opaque grains occurring as separate clasts and in lithic fragments, and the degree of weathering of the two is not very different. However, the opaque-mineral population in this sample must contain a significantly larger proportion of magnetite than the other samples in this group.

98DAP-201A

The fossils in this graywacke are calcareous shell fragments as much as 1.4 mm in length or diameter. The other clasts range in size from a maximum of 0.9 mm (generally volcanic lithic fragments) down to ≤0.3 mm diameter (angular single-crystal quartz clasts). The clast population is largely derived from mafic volcanic rocks, and most of these clasts have been chloritized. Secondary chlorite has also grown into pores from clast surfaces. Some calcite fills veins and occurs as patches in plagioclase. The elongate shell fragments are aligned, and the largest calcite vein is sub-parallel to this fabric element. The sample contains a number of recent fractures, but it does not look significantly weathered.

98DAP-201B

Although nearly identical to 98DAP-201A, the fossils in this sample are a little smaller (1.2 mm maximum length for cross sections and ≈0.9 mm maximum diameter for views of the shell surface), whereas some of the volcanic clasts are larger (1.2 mm maximum length). In addition, bedding is somewhat better defined in this sample. It also has a larger calcite content, much of which partly replaces minerals such as plagioclase. Narrow calcite-filled veinlets are moderately abundant; they span approximately a 30° range of orientations at a large angle to the bedding. The sample also contains a series of recently formed, open fractures, and some of the extensive weathering of this sample is concentrated along the walls of these fractures.

98DAP-201C

Volcanic lithic fragments reach ≈1.25 mm diameter in this sample, similar to 98DAP-201B, but the fossil fragments are as long as 3 mm. Based on their shapes and textures, at least some of the chloritized mafic grains (Table 14) may have been pyroxenes. The chlorite in the matrix is a secondary mineral that grows into the pore spaces from clast surfaces. This sample contains one set of wide (to 1 mm), calcite-filled veins oriented sub-parallel to a bedding direction defined by the elongate fossil fragments, and a second vein set that is nearly perpendicular to the first. This sample does not have as many fresh, open fractures as 98DAP-201A or -201B, and those that are

present do not cross the entire sample. The splotchy weathering pattern, however, is similar to 98DAP-201A and -201B.

98DAP-202A

The clast content of this sample is similar to several of the other samples in this group, being dominated by mafic volcanic lithic fragments and plagioclase grains (Table 14). Its appearance is rather different, however, because of the extensive growth of secondary minerals, principally calcite and chlorite along with some opaque minerals and probably other sheet silicates. The volcanic lithic fragments largely consist of a dark, fine-grained matrix with plagioclase laths of various sizes and abundances. A few of these lithic fragments also contained euhedral pyroxene phenocrysts. Plagioclase grains are the next most abundant clast type, and some of these are among the largest grains in the rock, at ≈1.4 mm diameter. A few elongate opaque grains reach 1.7 mm in length and 0.3 mm width. Clasts typically have low sphericity but are moderately rounded. The minor quartz in the sample is concentrated in the plutonic and quartzose metasedimentary clasts, as was also the case with 98DAP-0030 and 98DAP-201B (Table 14). This is the only sample in this group of eight that lacked anything resembling a fossil fragment.

The plagioclase content reported in Table 14 reflects the original detrital make-up of this sample, because nearly all of the plagioclase has been replaced by calcite, with some chlorite and possibly other sheet-silicate minerals such as kaolinite. The best preserved plagioclase crystals are found in the rare plutonic igneous fragments; these crystals may have been preserved because they have lower anorthite contents than either the plagioclase clasts or the plagioclase laths in the volcanic lithic fragments. The lithic fragments have also been heavily chloritized. The interstitial areas between grains are filled with secondary minerals, giving the sample a very closely packed appearance. Typically, a thin dusting of opaque minerals lines the rim of a clast (particularly if it is a mafic volcanic clast), and outside that is a 7–8 μm-thick band of chlorite. Nearly every clast is surrounded by a band of chlorite. Where the pore spaces are wider, the centers are filled with calcite or aggregates of chlorite. Some of the chlorite in the lithic fragments also has grown in narrow bands, making it hard to distinguish clasts from matrix in several cases.

No suggestion of bedding was seen. The sample contains one prominent calcite-filled vein that crosses the thin section and a few narrower ones oriented at about a 15° angle to the principal one. Short, thin, discontinuous calcite veinlets have no preferred orientation. The large calcite vein has refractured along one side, and the few traces of weathering in this sample are concentrated along that break.

98DAP-208

This is a tightly packed graywacke with irregularly shaped clasts. The largest fossil is 1.75 mm long and the largest lithic fragment ≈1.25 mm long, with grain sizes evenly distributed downwards. No suggestion of bedding planes was observed, but this may be a function of the thin-section orientation: most of the fossil fragments show the shell surface rather than cross-sections, indicating that the thin section was cut parallel to bedding. Although generally similar to the three 98DAP-201 samples, this rock has a darker appearance in plane polarized light, due to the abundance of aphanitic volcanic and shaly detritus and of Fe-oxides. Nevertheless, there are also many dacitic volcanic clasts consisting principally of fine-grained feldspar and quartz.

In fact, the sample contains more quartz clasts than any of the samples in this group except 98R-112 (Table 14). A few of the chloritized mafic grains may originally have been olivine. The Fe-oxides occur as clasts, as exsolved secondary minerals in chloritized grains, and in the graywacke matrix. Calcite is abundant as a matrix mineral, as a partial replacement of plagioclase, and as a fracture-filling mineral. One of the calcite veins has refractured, and some narrow, irregular open cracks are also present. Much of the chlorite in the sample has a reddish, weathered overprint.

Fine-grained Graywackes

(Samples: 98HAY-051 and 98HAY-051B.)

Table 15. Clast Content and Physical Properties of Fine-Grained Graywackes

	98HAY-051A	98HAY-051B
Lithic Fragments		
Volcanic	6.0	7.3
Metasedimentary	3.1	4.0
Sedimentary	7.5	8.1
Single-crystal Clasts		
Quartz	31.0	32.6
Plagioclase	9.2	11.2
K-feldspar	9.8	13.1
Biotite	4.4	6.7
Chlorite*	3.3	3.7
Muscovite	2.1	0.6
Opaques/heavy minerals	1.9	1.5
Calcite	1.3	—
Matrix	20.4	11.2
Total	100.0	100.0
Grain Density (g/cm^3)	2.61	2.47
Sat. Bulk Density (g/cm^3)	2.55	2.38
Dry Bulk Density (g/cm^3)	2.51	2.33
Susceptibility (cgs x 0.001)	0.01	0.01

*Mostly replaces biotite.

98HAY-051A

This graywacke has a reasonably high quartz content (Table 15), and it somewhat resembles a finer-grained version of H114 because of the presence of biotite, K-feldspar, and muscovite. A number of elongate, narrow quartz clasts reach 0.35 x 0.03 mm in size, and some biotites are as large as 0.60 x 0.05 mm. These elongate clasts define a bedding direction. The more equant clasts do not exceed ≈0.35 mm diameter.

All of the calcite appears to be secondary, occurring in part as a replacement of feldspar and other clasts but principally as a pore-filling mineral in the matrix. Grain boundaries are partly obscured by overgrowths from the matrix that, along with the calcite, include chlorite, opaque minerals, possible leucoxene, and phengitic white mica. No intergranular fractures are present, and very few clasts contain intragranular or transgranular cracks. Some of the Fe-oxides have red haloes, indicating some weathering.

98HAY-051B

This sample is slightly darker than 98HAY-051A, because of its somewhat greater abundance of biotite and volcanic lithic fragments (Table 15). It also contains very little calcite, which is a prominent matrix mineral in 98HAY-051A, although one ≈8-mm diameter area does contain splotches of calcite both in the matrix and in plagioclase clasts. The small amount of pore-filling calcite may also explain the slightly lower density of this sample compared to 98HAY-051A. A number of lithic fragments are quartzose, either quartz-rich sedimentary or metasedimentary rocks or felsic volcanics. Bedding is suggested by the alignment of long, narrow clasts (maximum length ≈0.36 mm) as in 98HAY-051A, but elongate clasts are less abundant in this sample. The largest relatively equant grains are ≈0.34 mm in diameter. There are no intergranular cracks, but the ends of some of the long, narrow quartz clasts are broken and a few intragranular cracks follow the cleavages in feldspar clasts. This sample has a strong reddish cast — the red color being concentrated along grain boundaries — and it probably is somewhat more weathered than 98HAY-051A.

The very low susceptibility values of both samples are consistent with their small proportions of volcanic lithic fragments (Table 15); those Fe-oxide minerals that are present have probably been oxidized during weathering.

References

Deer, W. A., Howie, R. A., and Zussman, J., 1962, *Rock-Forming Minerals, Vol. 2, Chain Silicates*, John Wiley and Sons Inc., New York, 379 pp.

Deer, W. A., Howie, R. A., and Zussman, J., 1962, *Rock-Forming Minerals, Vol. 3, Sheet Silicates*, John Wiley and Sons Inc., New York, 270 pp.

Deer, W. A., Howie, R. A., and Zussman, J., 1962, *Rock-Forming Minerals, Vol. 4, Framework Silicates*, John Wiley and Sons Inc., New York, 435 pp.

Deer, W. A., Howie, R. A., and Zussman, J., 1966, *An Introduction to the Rock-Forming Minerals*, John Wiley and Sons Inc., New York, 528 pp.

Graymer, R. W., 2000, Geologic map and digital database of the Oakland metropolitan area, Alameda and Contra Costa Counties, California, *U. S. Geological Survey Miscellaneous Field Studies Map MF-2342*, 29 pp., 1 sheet, scale 1:50,000.

Lienkaemper, J. J., Borchardt, G., and Lisowski, M., 1991, Historic creeprate and potential for seismic slip along the Hayward fault, California, Journal of Geophysical Research, vol. 96, pp. 18,261–18,283.

Moore, D. E., 1997, Mineralogical and microstructural investigations of core samples from the vicinity of the Great Sumatran fault, Indonesia, *U. S. Geological Survey Open-File Report 97-694*, 112 pp.

Moore, D. E., and Liou, J. G., 1979, Chessboard-twinned albite from Franciscan metaconglomerates of the Diablo Range, California, *American Mineralogist*, vol. 64, pp. 329-336.

Moore, D. E., Lockner, D. A., Ito, H., and Ikeda, R., 2000, Correlation of deformation textures and laboratory measurements of permeability and strength of Nojima fault zone core samples, *U. S. Geological Survey Open-File Report 00-129*, pp. 159-165.

Morrow, C. A., and Lockner, D. A., 2001, Hayward fault rocks: Porosity, density, and strength measurements, *U. S. Geological Survey Open-File Report 01-*, in review.

O'Hanley, D. S., 1996, *Serpentinites, Records of tectonic and Petrological History*, Oxford University Press, Oxford, England, 277 pp.

Ponce, D., Hildenbrand, T., Jachens, R., Roberts, C., and Fahringer, P., 1998, gravity and magnetic anomalies along the Hayward fault and their relation to earthquake seismicity, California, *Eos, Transactions American Geophysical Union*, v. 79, p. F594.

Appendix

Locations of Samples Collected for Physical Property Measurements

Sample Number	Latitude* deg	min	Longitude* deg	min	Notes
Igneous Rocks					
H101	37	39.85	122	3.91	Gabbro, Jgb**
H103	37	42.79	122	6.64	Gabbro, Jgb
98R-108	37	39.21	122	3.01	Gabbro, Jgb
98DAP-001	37	43.32	122	6.57	Gabbro, Jgb
98DAP-006A	37	39.79	122	3.94	Gabbro, Jgb
98DAP-006B	37	39.79	122	3.97	Gabbro, Jgb
98DAP-007	37	39.84	122	4.04	Gabbro, Jgb
98DAP-207	--	--	--	--	Gabbro, Jgb
H107	37	38.70	122	3.06	Basalt
98DAP-206A	37	38.37	122	2.44	Tonalite
98DAP-205	37	38.32	122	2.49	Tonalite/Diorite
98DAP-206B	37	38.37	122	2.44	Tonalite/Diorite
H102	37	41.24	122	5.14	Keratophyre (“altered’), Jsv
H111	37	45.94	122	8.98	Keratophyre, Jsv
98DAP-002	37	43.32	122	6.57	Serpentinized Peridotite
97HAY-317	37	47.96	122	10.64	Serpentinized Clinopyroxenite
Sedimentary Roc					
H114	37	45.51	122	7.30	Joaquin Miller Formation, Kjm
98R-113	37	45.53	122	7.32	Kjm
98R-110	37	39.95	122	3.23	Kjm
98DAP-209A	37	38.35	122	2.60	Volcanic-rich Conglomeratic Rock
98DAP-209B	37	38.35	122	2.60	Volcanic-rich Conglomeratic Rock
98DAP-209C	37	38.35	122	2.60	Volcanic-rich Conglomeratic Rock
98R-105	37	38.71	122	3.07	Knoxville Sandstone, volcanic breccia member, KJkv
98R-112	37	45.47	122	8.24	Knoxville Sandstone, conglomerate member, KJkc
98DAP-0030	37	37.94	122	2.09	KJkv
98DAP-201A	37	38.45	122	2.60	Graywacke
98DAP-201B	37	38.45	122	2.60	Graywacke
98DAP-201C	37	38.45	122	2.60	Graywacke
98DAP-202A	37	38.40	122	2.57	Graywacke
98DAP-208	37	38.41	122	2.57	Graywacke
98HAY-051A	37	43.54	122	6.07	Fine-grained Graywacke
98HAY-051B	37	43.54	122	6.07	Fine-grained Graywacke

*North American Datum 1927 (NAD27); **Unit labels from Graymer (2000).